Landslides induced by the interaction of an earthquake and subsequent rainfall. A spatial and temporal model

Glissements de terrain induits par l'interaction d'un tremblement de terre suivi de précipitations. Un modèle spatio-temporel

Quan Luna B., Vangelsten B.V., Liu Z.Q., Eidsvig U., Nadim F.
Norwegian Geotechnical Institute (NGI) / International Centre for Geohazards (ICG), Norway

ABSTRACT: The consideration of multiple hazards and their interaction to achieve risk reduction is a necessity since many regions are prone to different types of threats. However, this is neither simple and straightforward nor commonly undertaken at present since different natural hazards are usually analyzed individually and managed separately. A common example of this is the alteration of the density and locations of rainfall-induced landslides after an earthquake due to the extensive disturbance of surface strata. That implies an influence of the earthquake on the soil structure that alters the disposition towards landslides. Taking this into consideration, a model was developed that could give a rough spatial and temporal prediction of expected change in landslide hazard in an area following an earthquake. The model is able to describe the reduced impact of earthquakes with distance from epicentre as well as how the soil gradually regains its strength with time. These reductions are then applied to an equilibrium stability analysis in order to compute new Factors of Safety. Although analysis schemes can be proposed and software tools can be provided to facilitate many steps, a well-conceived and reflective approach to multi-hazard settings is still essential.

RÉSUMÉ : Etant donné que différentes régions sont sujettes à différent types de menace, l'étude de multiples facteurs de risque et de leur interaction est nécessaire afin de réduire le risque. Ce genre d'études est néanmoins rarement entrepris de nos jours puisque chaque risque naturel est usuellement analysé et traité séparément. Un exemple courant est l'évolution de la densité et de la localisation des glissements de terrain induits par des précipitations suite à un tremblement de terre en raison de l'importante perturbation des couches superficielles. Cela implique que l'influence des tremblements de terre sur la structure du sous-sol modifie la prédisposition aux glissements de terrain. Compte de tenu de cela, un modèle de prédiction spatio-temporelle de la variation du risque de glissement de terrain dans une région donnée suite à un tremblement de terre a été développé. Le modèle est capable de décrire la diminution de l'impact des tremblements de terre en fonction de la distance à l'épicentre ainsi que la manière dont le sous-sol retrouve sa résistance initiale. Ces diminutions sont ensuite appliquées à une analyse de stabilité de façon à calculer de nouveaux facteurs de sécurité. Bien que des programmes d'analyses puissent être proposés et que des logiciels peuvent être fournis afin de faciliter de nombreuses étapes, une approche réfléchie et bien conçue des environnements à dangers multiples reste indispensable.

KEYWORDS: Landslide, Earthquake, Rainfall, Slope stability, Factor of Safety

1 INTRODUCTION

A multi-hazard analysis refers to the implementation of methodologies and approaches aimed at assessing and mapping the potential occurrence of different types of natural hazards in a given area. Analytical methods and mapping have to take into account the characteristics of the single hazardous events as well as their mutual interactions and interrelations (Delmonaco et al. 2006). The existence of relations between natural hazards and the potentially resulting consequences is an issue of increasing importance in multi-hazard studies (Kappes et al. 2010). The specific methods to deal with related hazards are as diverse as the terms and the phenomena falling into this category. However, a general approach can be applied where the investigation of the individual chain of one hazard triggering the next is performed (so-called cascading events).

Evidently, performing multi-hazard risk analysis is not a simple operation. Apart from the data requirements and time-consuming conduction of single-hazard risk studies that require know-how from different disciplines, many further aspects have to be considered. One important source of difficulty is the contrast in hazard characteristics. Hazards differ with respect to their properties such as time of onset, duration, physical properties and extent. As a result, the modelling approaches adjusted to the hazard specifics also contrast strongly (Bovolo et al 2009).

2 MODEL DESCRIPTION

The proposed model aims to compute and estimate the associated alteration in the landslide hazard following an earthquake event. The model describes the reduced impact of earthquakes with distance from epicentre as well as how the soil gradually regains its strength with time. This was achieved by analyzing the collected data on how seismic activity influences the critical rainfall intensity and duration needed to trigger landslides in the area impacted by the earthquake. Based on the gathered information the modelling objective was met by constructing three sub-models: A) Use empirical data to construct a sub-model linking rainfall threshold reduction as function of time after earthquake impact; B) Use empirical data to construct a sub-model linking rainfall threshold reduction as function of distance from epicentre and earthquake magnitude, C) Use an analytical hydrological model to link rainfall threshold reduction to changes in soil shear strength.

Sub-models A and B together form an empirical model for rainfall threshold reduction as a function of magnitude, distance and time after the earthquake. The model is based on the following assumptions:

- The effect of earthquake on the rainfall threshold reduction decays with distance from and time after the earthquake.
- The maximum rainfall threshold reduction (i.e. rainfall threshold reduction immediately after and at epicenter) is assumed to be a function of earthquake magnitude only.

- The temporal and spatial effects are independent and thus the spatial and temporal variations are treated separately in two different functions and multiplied to find the actual rainfall threshold reduction.
- The earthquake effect is included into the spatial model. The temporal model is a normalized model representing the remaining threshold reduction as a function of time after the earthquake.

According to the assumptions above, the threshold reduction for a given point in time and space is a product of the spatial model and the temporal model (Eq. 1):

$$\text{Threshold reduction } (X, T, M) = f_{spatial}(X, M) \cdot f_t(T) \quad \text{Eq.(1)}$$

In this model, X is the distance to the epicenter, T is the time after the earthquake and M is the earthquake magnitude. The purpose of the model is to relate the post-earthquake rainfall threshold to the pre-earthquake threshold using the derived threshold reduction function (Eq. 2):

$$\text{Post-earthquake threshold} = (1 - \text{Threshold reduction}(X, T, M)) \cdot \text{Pre-earthquake threshold} \quad \text{Eq.(2)}$$

The rainfall threshold changes referred to in the model is the numerical value of the mean rainfall intensity for a duration of one hour, i.e. α in Eq. 3 below:

$$I = \alpha D^{\beta} \quad \text{Eq.(3)}$$

In this equation, I is the mean rainfall threshold intensity, D is the rainfall duration in hours and β is the slope of the threshold curve in log-log space.

2.1 *Rainfall threshold reduction as function of time*

Shou et al. (2011) modelled the effect of earthquake on the rainfall threshold reduction by an exponentially decaying function with time. The model parameter could be transferred to cumulative precipitation by using the annual mean precipitation. In the proposed model, the variations caused by other relevant parameters, such as slope angle and actual precipitation, are not treated explicitly; but model uncertainty is added to account for such variations. Shou et al. (2011) provided some data on the temporal effect of the Chi-Chi earthquake. No such data exist for the Wenchuan earthquake. From the available data it appears that the temporal behavior is site-dependent. However, Shou et al. (2011) used a model representing the average of three sites in Taiwan. Model uncertainty was introduced by two curves representing uncertainty bands. The uncertainty bands represent deviations of ±50% from the average curve in a semi-log coordinate system.

Figure 1 shows the variation of the normalized rainfall threshold reduction with time for three different locations in Taiwan together with the average curve and uncertainty bands. The figure illustrates the long-term effects after the Chi-chi earthquake.

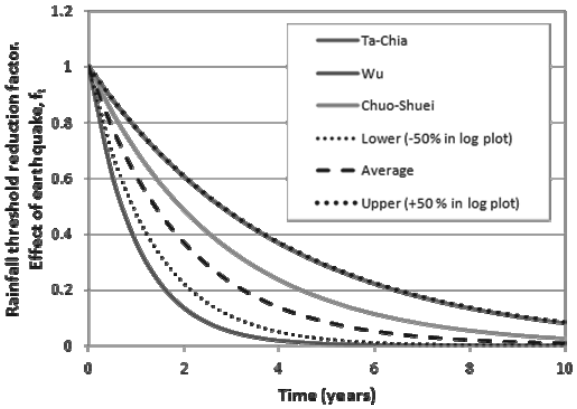

Fig. 1 Remaining rainfall threshold reduction (i.e. rainfall threshold reduction factor) as a function of time for three locations in Taiwan (colored curves) as well as an average curve and curves representing model uncertainty (black curves).

2.2 *Rainfall threshold reduction as function of distance and earthquake magnitude*

The rainfall threshold reduction as a function of earthquake magnitude and distance from the epicenter is based on the following relations and assumptions:

- For the spatial variation, the effect of earthquake on the rainfall threshold reduction is assumed to decay exponentially with distance from the epicenter/fault. This assumption is based on observations after the Chi-Chi earthquake by Khazai & Sitar (2003).
- The maximum "influence radius" of an earthquake is a function of the magnitude. The function described by Keefer (1984) is applied. This function describes the maximum distance from epicenter for seismically induced landslides as a function of earthquake magnitude. It was further assumed that at for a distance equal to the influence distance of the earthquake, the rainfall threshold reduction was 1/100 of the rainfall threshold reduction at distance 0.
- The model for maximum rainfall threshold reduction as a function of magnitude is assumed to increase with increasing magnitude.

Based on the above mentioned relations, a conceptual model for rainfall threshold reduction as a function of earthquake magnitude and distance from epicenter may be established as illustrated in Figure 2.

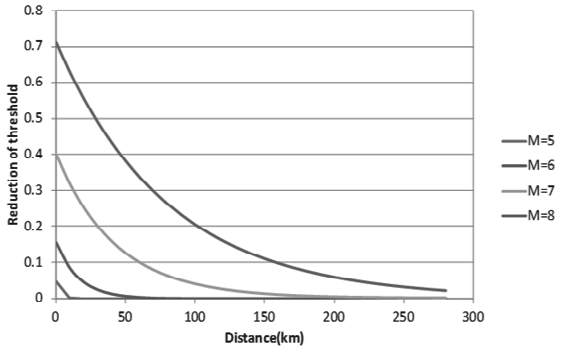

Fig. 2 Reduction of rainfall threshold caused by earthquake as a function of magnitude and distance

2.3 *Linking rainfall threshold reduction and reduction of soil shear strength*

Post-earthquake soil strengths may be lower than pre-earthquake (static) strengths for zones that are susceptible to

strength loss. As time passes, the progression of soil self-healing will result in increased shear strength compared to shortly after the earthquake. Temporal changes of soil properties are known to have an effect on the rainfall thresholds required to trigger landslides (Tang et al. 2009). Due to the decreased soil strength, landslide-triggering rainfall thresholds decrease compared with their pre-earthquake values (Lin et al. 2004).

A proposed methodology is presented for estimating temporal changes in soil strength related to landslide-triggering rainfall thresholds after an earthquake over a wide area (a few square kilometers). This methodology is based on response analysis with a deterministic, spatially distributed model that combines a 1-D transient infiltration model with a safety-factor analysis for calculating rainfall threshold.

After an earthquake, an abundance of loose landslide debris can be present on the hillslopes. The potential failure surface typically lies at or near the contact between the relatively permeable colluvium and the relatively impermeable underlying bedrock. The thickness of the soil cover is small compared with the length of slope, thus the infinite slope stability model can be performed to evaluate slope stability. Limit equilibrium conditions are reached at a certain depth when the mobilized shear stress (a function of soil unit weight, failure surface depth and slope angle) equals the soil shear strength, given by the Mohr-Coulomb failure criterion (Eq. 4):

$$\frac{\tan\phi'}{\tan\alpha}+\frac{c'-\gamma_w\psi\tan\phi'}{\gamma_s d_b\sin\alpha\cos\alpha}=1 \qquad \text{Eq.(4)}$$

where c' and φ are the effective cohesion and friction angle of the soil, d_b is the depth of the failure surface, α is the slope angle, γ_s is the soil unit weight γ_w, is the specific weight of water, and ψ is the pressure head at the failure surface.

The limiting value of the pressure head which leads a slope with given geometrical characteristics and soil properties to limit equilibrium conditions can be calculated from Equation 5 as:

$$\psi_{\lim}=\frac{c'}{\gamma_w\tan\phi'}+\frac{\gamma_s}{\gamma_w}d_b\cos^2\alpha\left(1-\frac{\tan\alpha}{\tan\phi'}\right) \qquad \text{Eq.(5)}$$

For a saturated soil cover, the evolution of the pressure head with time and depth inside the slope is governed by the following one-dimensional conservation equation (Eq. 6) (Iverson 2000):

$$\frac{\partial\psi}{\partial t}=D\frac{\partial^2\psi}{\partial Z^2} \qquad \text{Eq.(6)}$$

where Z is the depth of the point considered with respect to an horizontal reference plane; $D=D_0/\cos^2\alpha$ and D_0 is the hydraulic diffusivity of the soil.

Two factors, *fs* and *fi*, which are respectively reduction factors of soil shear strength and critical rainfall intensity, are now introduced. It is assumed that the effective cohesion and tangent of effective internal friction angle have the same reduction factor *fs*. The reduction factor of critical rainfall intensity is calculated by dividing the reduced rainfall intensity $I_{reducrit}$ due to soil shear strength reduction by the original critical rainfall intensity I_{critic} (Eq. 7):

$$f_I=\frac{I_{Reducrit}}{I_{crit}} \qquad \text{Eq.(7)}$$

For sandy soil, where the cohesion is zero, i.e. c = 0, an approximation solution is given by Eq. 8:

$$f_I=\frac{\frac{\gamma_s}{\gamma_w}d_b\left(1-\frac{\tan\alpha}{f_S\tan\phi'}\right)-\left(d_b-d_w\right)}{\frac{\gamma_s}{\gamma_w}d_b\left(1-\frac{\tan\alpha}{\tan\phi'}\right)-\left(d_b-d_w\right)} \qquad \text{Eq.(8)}$$

3 RESULTS

3.1 *Study area: MATRIX virtual region*

The case presented below is used to demonstrate the capabilities of the model in terms of hazard assessment. It is not a validation of the performance of the model. The case partly makes use of artificial data (including the digital elevation model) and partly typical engineering values (as for the soil parameters and rainfall intensity). A digital elevation model (DEM) has been developed for demonstration of the landslide hazard model (Fig. 3)

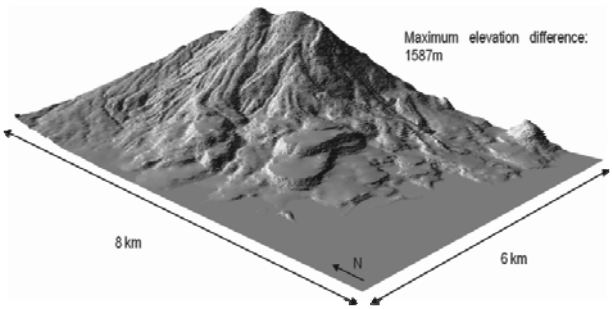

Fig. 3 3D representation of digital elevation model (DEM) for the case study region.

3.2 *Reduction factor for critical rainfall intensity*

Figure 4 shows the results of the reduction factor inside the virtual region for a sandy soil where the earthquake event has a magnitude of 6.98 with a fault length of 3.08 km. The time span after the earthquake is assumed to be 45 days.

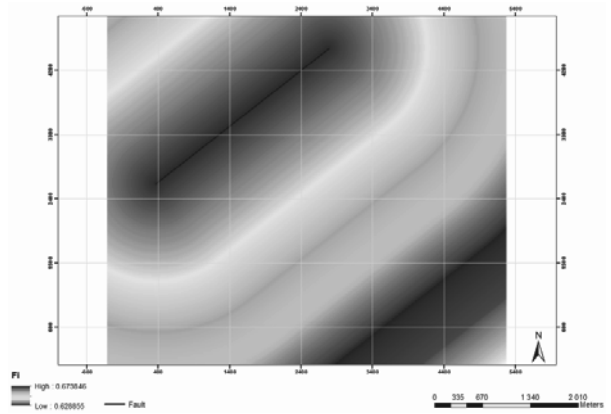

Fig. 4 Rainfall threshold reduction factor *(fi)* as a function of time, magnitude and distance to the fault.

The temporal model represents the remaining threshold reduction as a function of time after the earthquake. The remaining threshold reduction is represented by a normalized function with values between 0 and 1. Value 1 corresponds to the maximum rainfall threshold reduction (i.e. the rainfall threshold reduction immediately after the earthquake) and value 0 corresponds to no remaining rainfall threshold reduction (i.e. after long time, when the occurrence of the earthquake has no effect on the rainfall threshold.) The effect from the earthquake on the rainfall threshold reduction is included in the spatial model.

3.3 *Reduction factor of the soil shear strength*

A quantitative assessment of the relationships between different factors (i.e. slope angle, failure depth and water table depth) and reduction factor of soil shear strength due to earthquake was performed. Figure 5 shows the areal distribution of the reduction factor of the soil shear strength considering a rainfall intensity of 120 mm a day. The bedrock is assumed to be much less permeable than the soil cover. Soil depth varies from 4 to 7 m depending on the type of soil and topographic characteristics inside the virtual region.

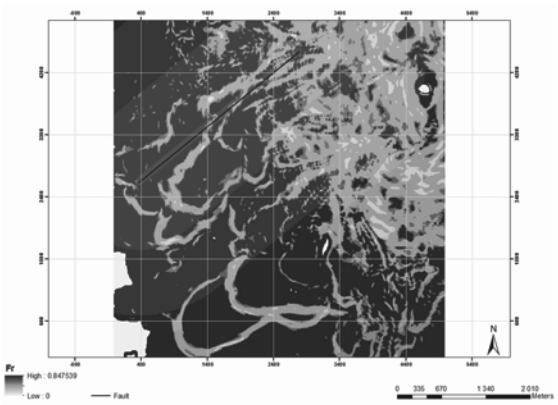

Fig. 5 Spatial distribution of the soil shear strength reduction factor *(fr)*.

3.4 *Slope stability assessment including the reduction factors*

A two dimensional equilibrium stability analysis based on the infinite slope model was carried out in order to compute the new factors of safety that included the reduction factors. The mean values of the logarithmic distributions functions of the input parameters were applied in the analyses. A constant porosity of 42% and an evapotranspiration of 5 mm/day were selected throughout the area. Five different friction angles were used for the different soil types: 30, 32, 34, 36, 38°. Figure 6 shows the results of the stability analysis considering the reduction of the soil strength after an earthquake.

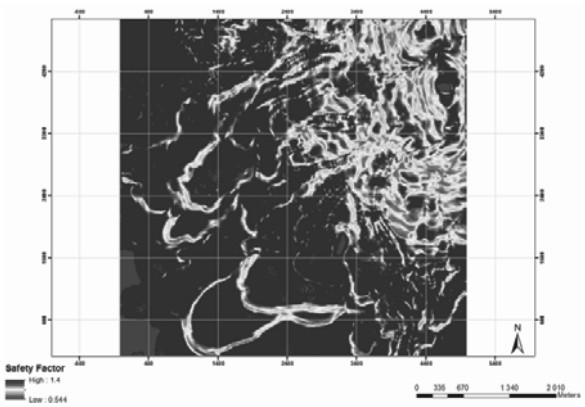

Fig. 6 Stability analysis considering the loss of strength of soil due to the perturbations caused by a magnitude 6.98 earthquake.

4 CONCLUSIONS

A natural system is not just the sum of its components but is the result of many interacting parts. Hence, a multi-hazard assessment should address evolving characteristics in space and time. These characteristics can, for analysis purposes, be analyzed as the alteration of the susceptibility and the triggering mechanism. A multi-hazard assessment offers the advantage to consider a slightly larger part of the overall system. The major challenge is to identify the relationships among the interacting factors and establish the respective links.

For this reason, a model that includes the reduction of the soil strength parameters induced by the strong motion of an earthquake was developed and implemented. A virtual case study was performed to assess the behavior of the model and its parameters. This was achieved by calculating two reduction factors that represented the reduction of rainfall threshold in space and time, and the reduction of the soil strength due to prevailing conditions.

There are still some limitations regarding the model and further validation needs to be done. A thorough calibration of the reduction factors should be done locally and the possibility of using real events that are well documented should be considered. However, despite its limitations, the model provides a practical approach to assess the prospective outcomes of future hazards and their interactions. Thus the model contributes to increasing the knowledge required for the protection of the people at risk and their assets.

5 ACKNOWLEDGEMENTS

The research leading to these results has received funding from the European Community's Seventh Framework Programme [FP7/2007-2013] under Grant Agreement No 265138 New Multi-HAzard and MulTi-RIsK Assessment MethodS for Europe (MATRIX).

6 REFERENCES

Bovolo, C. I., Abele, S. J., Bathurst, J. C., Caballero, D., Ciglan, M., Eftichidis, G., Simo, B. 2009. A distributed framework for multi-risk assessment of natural hazards used to model the e_ects of forest _re on hydrology and sediment yield. *Computers & Geosciences* 35(5): 924 - 945.

Delmonaco, G., Margottini, C., Spizzichino, D. 2006. ARMONIA methodology for multi-risk assessment and the harmonisation of different natural risk maps. *Deliverable 3.1.1, ARMONIA*

Iverson, R. M. 2000. Landslide triggering by rain infiltration. *Water Resources Research*, 36(7), 1897-1910.

Kappes, M., Keiler, M., Glade, T. 2010. From single- to multi-hazard risk analyses: a concept addressing emerging challenges. In Malet, J.-P., Glade, T. & Casagli, N. (Eds.), *Mountain Risks: Bringing Science to Society*. Proceedings of the International Conference, Florence. CERG Editions, Strasbourg, 351-356.

Keefer, D. K. 1984. Landslides caused by earthquakes. *Geological Society of America Bulletin*, v 95, pp. 406 – 421.

Khazai, B., Sitar, N. 2003. Evaluation of factors controlling earthquake-induced landslides caused by Chi-Chi earthquake and comparison with the Northridge and Loma Prieta events. *Engineering Geology*, 71, pp. 79 - 95.

Lin, C.W., Shieh, C. L., Yuan, B. D., Shieh, Y. C., Liu, S. H., and Lee, S. Y. 2004. Impact of Chi-Chi earthquake on the occurrence of landslides and debris flows: example from the Chenyulan River watershed, Nantou, Taiwan. *Engineering Geology*, 71, 49-61

Shou, K. J., Hong, C.Y., Wu, C.C., Hsu, H. Y., Fei, L. Y., Lee, J. F., Wei, C. Y. 2011. Spatial and temporal analysis of landslides in Central Taiwan after 1999 Chi-Chi earthquake. *Engineering Geology,* 123, pp. 122 – 128.

Tang, C., Zhu, J., Li, W. L. 2009. Rainfall-triggered debris flows following the Wenchuan earthquake. *Bulletin of Engineering Geology and the Environment,* 68, 187-194.